

Microscopic visualization of testosterone in mouse testis by use of imaging mass spectrometry

Shuichi Shimma¹ · Henri-Obadja Kumada² · Hisanori Taniguchi^{2,3} · Alu Konno^{4,5} · Ikuko Yao^{2,4,5} · Kyoji Furuta⁶ · Tadashi Matsuda³ · Seiji Ito²

Received: 5 January 2016 / Revised: 16 April 2016 / Accepted: 20 April 2016 / Published online: 26 May 2016
© Springer-Verlag Berlin Heidelberg 2016

Abstract Testosterone is one of the androgens synthesized from cholesterol as a precursor in the Leydig cells of testes. Since the ionization efficiency of testosterone in matrix-assisted laser desorption/ionization (MALDI) is quite low, visualization of testosterone by using MALDI-imaging mass spectrometry (MALDI-IMS) has

been considered difficult. To overcome this problem, we used two types of on-tissue derivatization techniques, which were achieved by pyridine sulfur trioxide and Girard's T (GT) reagent, to introduce a polar group into testosterone molecule with the aim to increase the sensitivity. Derivatization by use of GT reagent provided excellent results, superior to those obtained with pyridine sulfur trioxide, in terms of ionization efficiency, molecular specificity, and tissue damage. In GT derivatized testis tissues of mice treated with human chorionic gonadotropin (hCG), testosterone was broadly observed both inside and outside the seminiferous tubules by using an iMScope. To evaluate our imaging results, we performed quantification experiments of underivatized testosterone extracted from hCG-treated testes and control testes using LC-MS/MS. We confirmed the 256-fold concentration change between hCG-treated tissues and control tissues. We also confirmed the 228-fold change in detected peak intensities between hCG-treated tissue sections and control tissue sections in imaging results. We consider our tissue preparation methods for IMS provide high sensitivity with high precision. In addition, high-spatial definition IMS was also available, and we confirmed testosterone had mainly accumulated on the surface of the Leydig cells.

Published in the topical collection *New Applications of Mass Spectrometry in Biomedicine* with guest editors Mitsutoshi Setou and Toshimitsu Niwa.

Shuichi Shimma and Henri-Obadja Kumada contributed equally to this work.

Electronic supplementary material The online version of this article (doi:10.1007/s00216-016-9594-9) contains supplementary material, which is available to authorized users.

✉ Seiji Ito
ito@hirakata.kmu.ac.jp

¹ Division of Advanced Science and Biotechnology, Graduate School of Engineering of Osaka University, 2-1 Yamadaoka, Suita, Osaka 565-0871, Japan

² Department of Medical Chemistry, Kansai Medical University, 2-5-1 Shin-machi, Hirakata, Osaka 573-1010, Japan

³ Department of Urology and Andrology, Kansai Medical University, 2-5-1 Shin-machi, Hirakata, Osaka 573-1010, Japan

⁴ Department of Optical Imaging, Institute for Medical Photonics Research, Preeminent Medical Photonics Education & Research Center, Hamamatsu University School of Medicine, 1-20-1 Handayama, Higashi-ku, Hamamatsu, Shizuoka 431-3192, Japan

⁵ JST, ERATO, Sato project, Tokyo 160-8582, Japan

⁶ Regeneration and Advanced Medical Science, Gifu University Graduate School of Medicine, Yanagido 1-1, Gifu, Gifu 501-1193, Japan

Keywords Imaging mass spectrometry · iMScope · Testosterone · Testis · Derivatization · Girard's T reagent

Abbreviations

GT Girard's T reagent
GT-Ts Girard's T derivatized testosterone
IMS Imaging mass spectrometry
MALDI Matrix-assisted laser desorption/ionization

Ts	Testosterone
TsS	Testosterone sulfate ester
α -CHCA	α -Cyano-4-hydroxycinnamic acid

Introduction

Testosterone synthesized in Leydig cells of testes is the principal mammalian androgen and is essential for spermatogenesis. Synthesized testosterone is promptly released into the bloodstream and acts on target cells in testes and other organs through androgen receptors [1].

Concentrations of testosterone in testes, testicular fluid, and serum have been conventionally measured by using quantitative immunoassay or mass spectrometry (MS) following extraction and/or chromatography to obtain accurate quantitative data [2–4]. By applying this technique, the intratesticular concentration of testosterone was shown to be 100–200 times greater than that of it in the serum [5]. However, extraction of testosterone precludes precise information on the spatial distribution of the molecule. Therefore, information about the pattern of testosterone release from Leydig cells and the distribution range of testosterone such as extending to Sertoli cells and seminiferous tubules remains unclarified.

To answer these questions, the application of recent mass spectrometric techniques such as imaging mass spectrometry (IMS) is promising [6]. However, when we use matrix-assisted laser desorption/ionization (MALDI)-based IMS, serious problems arise. One is the low ionization efficiency for low-polarity molecules such as cholesterol products including testosterone. Another is the image pixel size can be a limitation when we visualize molecular accumulation in cells. With respect to ionization efficiency, many techniques using derivatized steroid hormones and their application in liquid chromatograph (LC) MS analysis have been reported [7]. Although a few on-tissue derivatization methods to visualize neurotransmitters in whole brain sections using IMS have been reported [8–10], there are no reports on microscopic visualization of testosterone, because large matrix crystals via conventional matrix application procedures might interfere in images with small pixel size.

To obtain high ionization efficiency and high definition images while maintaining spatial precision after sample preparation, earlier we improved sample preparation procedures for MALDI experiments including on-tissue derivatization and two-step matrix application [11]. Furthermore, a new IMS instrument known as the iMScope has been recently developed to obtain imaging results with a micrometer pixel size. In this present study, we evaluated the use of the iMScope and on-tissue derivatization reagents for improvement of

ionization efficiency and accurate imaging of testosterone in testes.

Material and methods

Chemicals

Formic acid, acetic acid, acetonitrile, isopropanol, pyridine, and pyridine sulfur trioxide complex were purchased from Wako Pure Chemical (Osaka, Japan). α -Cyano-4-hydroxycinnamic acid (α -CHCA) of 99 % grade, Girard's T reagent (GT), d3-testosterone, and polyethylene glycole 400 (PEG400) were purchased from Sigma-Aldrich (St. Louis, MO, USA). Recombinant human chorionic gonadotropin (hCG) was supplied by ASKA Pharmaceutical Medical (Kanagawa, Japan). Indium-tin-oxide (ITO)-coated glass slides (100 Ω without MAS coating) were purchased from Matsunami Glass (Osaka, Japan).

Animal study

C57BL/6J male mice were purchased from SLC (Shizuoka, Japan). To induce testosterone production, we administered 5 μ L of hCG (500 IU) subcutaneously to the animals. The mice were anesthetized by sodium pentobarbital (i.p., 50 mg/kg) 60 min after the hCG treatment, and their testes were dissected and immediately frozen in powdered dry ice. All tissues were stored at -80 °C until use. All experimental procedures on animals were performed in accordance with the Guidelines of Japanese Association for Laboratory Animal Science and with the approval of the Animal Experimentation Committee at Kansai Medical University.

Tissue sectioning

Frozen 8- μ m sections were sliced at -20 °C with a cryomicrotome (Leica CM1950, Nussloch, Germany). To fix each tissue block on the tissue holder, we used an optimum cutting temperature (OCT) polymer. When the sections were generated, the cutting block was not embedded in OCT. Frozen sections were thaw-mounted on ITO-coated glass slides and allowed to dehydrate in a 50-mL conical tube containing silica gel. The glass slides placed in the conical tube were stored at -20 °C until derivatization.

On-tissue derivatization by use of pyridine sulfur trioxide

A pyridine sulfur trioxide solution of 66.7 mg/mL in pyridine was prepared, and 600 μ L of the solution was sprayed with an artistic airbrush (PS270, CREOS, Tokyo, Japan) onto each tissue surface repeatedly to avoid molecular migration due to residual derivatization solution. After all of the solution had

been dispensed, the tissue was put in a 100-mm culture dish containing wet cotton gauze and kept in an incubator at 55 °C for 2 h. For derivatization of a testosterone standard sample, 20 mg of testosterone and 120 mg of pyridine sulfur trioxide were mixed, and 1.8 mL of pyridine was then added. After sonication, the solution was kept at room temperature for 1 h for the reaction to occur.

On-tissue derivatization with GT

We optimized the on-tissue derivatization method using GT based on a previous report [8]. Although the conditions of the GT solution were evaluated in this research, we prepared the initial GT solution at 5.0 mg/mL in 2.5 % acetic acid and sprayed 50 µL of this solution onto each tissue surface using the artistic airbrush. After all of the solution had been dispensed, the tissue was kept at room temperature for 90 min. For derivatization of the testosterone standard sample, GT reagent was mixed in equal volume of testosterone standard sample, and kept for 10 min.

Matrix application

The two-step matrix application method was used as reported previously [11]. Tissue specimens in conical tubes containing silica gel were placed at room temperature for 10 min just before matrix deposition. For the first step, the glass slide bearing a specimen was removed from the tube and attached to a sample holder, which was then installed in a vacuum deposition system (SVC-700TMSG, Sanyu Electron, Tokyo, Japan). A matrix holder was filled with approximately 40 mg of α -CHCA powder, and the sample holder and matrix holder were positioned 8 cm apart. The vacuum pressure in the chamber was maintained at 10^{-4} Pa during the deposition. Subsequently, the α -CHCA was heated to 250 °C, the boiling point of the matrix crystals, and the vapor was deposited on the specimen surface for 8 min.

For the second step, α -CHCA (10 mg/mL) was dissolved in acetonitrile, isopropanol, and distilled water (all containing 0.1 % formic acid; FA) at a ratio of 3:1:6. The matrix solution (100 µL) was applied by use of an artist's airbrush (PS-270, GSI Creos, Tokyo, Japan). The distance between the tip of the airbrush and the tissue surface was 8 cm. For the first 3 cycles, the matrix was sprayed for 2 s at 60-s intervals, and for the subsequent 7 cycles, for 1.0 s at 30-s intervals.

IMS using an iMScope

Mass spectrometry was performed with the iMScope (Shimadzu, Kyoto, Japan) designed for IMS [12]. This instrument could provide taking optical pictures under microscopic views and ion distribution images within the same system. The laser spot size of approximately 12.5 µm (full-width

half maximum) was used as appropriate for the IMS experiment. Step sizes of 7 or 15 µm were used in this study. A laser irradiated the tissue surface with 50 shots (repetition rate; 1 kHz) for each pixel. Mass spectra were acquired in the positive ion detection mode for GT-Ts and negative ion detection mode for TsS by using an external calibration method with PEG400. In each experiment, the voltage of the detector was applied at a constant of 2.1 kV. Laser power and collision energy for MSⁿ experiments were optimized to maximize the ion intensity of product ions by reference to the derivatized standard testosterone samples. During a whole tissue scan, the measurement conditions maintained constant.

Quantification of testosterone using LC-MS/MS

Testes were prepared in the same manner as above. The weights of resected half pieces of testes were measured before freezing ($n = 3$ each hCG-treated and untreated). After frozen, testes were milled using a SK mill (SK-100G, Tokken, Chiba, Japan) followed by 1 mL addition of 100 % methanol into a tube for extraction. The 800-µL supernatant was collected into a new tube, and then 5 ng of d3-testosterone was spiked as an internal standard. A calibration curve was prepared by standard testosterone with internal standard. The solvents in the tissue sample and standard testosterone were completely evaporated with a rotary evaporator (CC-105, Tomy Seiko, Tokyo, Japan). The dried samples were dissolved in 500-µL of 100 % methanol, to become a final concentration of internal standard to 10 pg/µL. The dissolved samples were filtered (0.22 µm pore size) before LC-MS/MS measurement. The quantification was performed by Acquity (Waters, Milford, MA, USA) and 4000 QTRAP LC-MS/MS system (Sciex, Framingham, MA, USA).

Results

To enhance sensitivity for detection of testosterone, we first derivatized testosterone standard sample with GT or with pyridine sulfur trioxide. Figure 1 shows suggested structures of testosterone derivatives obtained with these two reagents. Testosterone sulfate (TsS) and Girard's T-testosterone (GT-Ts) have the sulfate group and trimethylamine group, respectively, and the ions were detected in mass spectra obtained from negative and positive ion detection modes, respectively. On the other hand, we performed measurement of non-derivatized testosterone to confirm the ionization efficiency in MALDI. Although the peak around m/z 289 was clearly observed in the mass spectrum (see Electronic Supplementary Material (ESM) Fig. S1a), the difference between it and the theoretical m/z was 0.13 Da. The obtained MS/MS spectrum of m/z 289.09 did not provide specific peaks derived from the testosterone structure (ESM Fig. S1b).

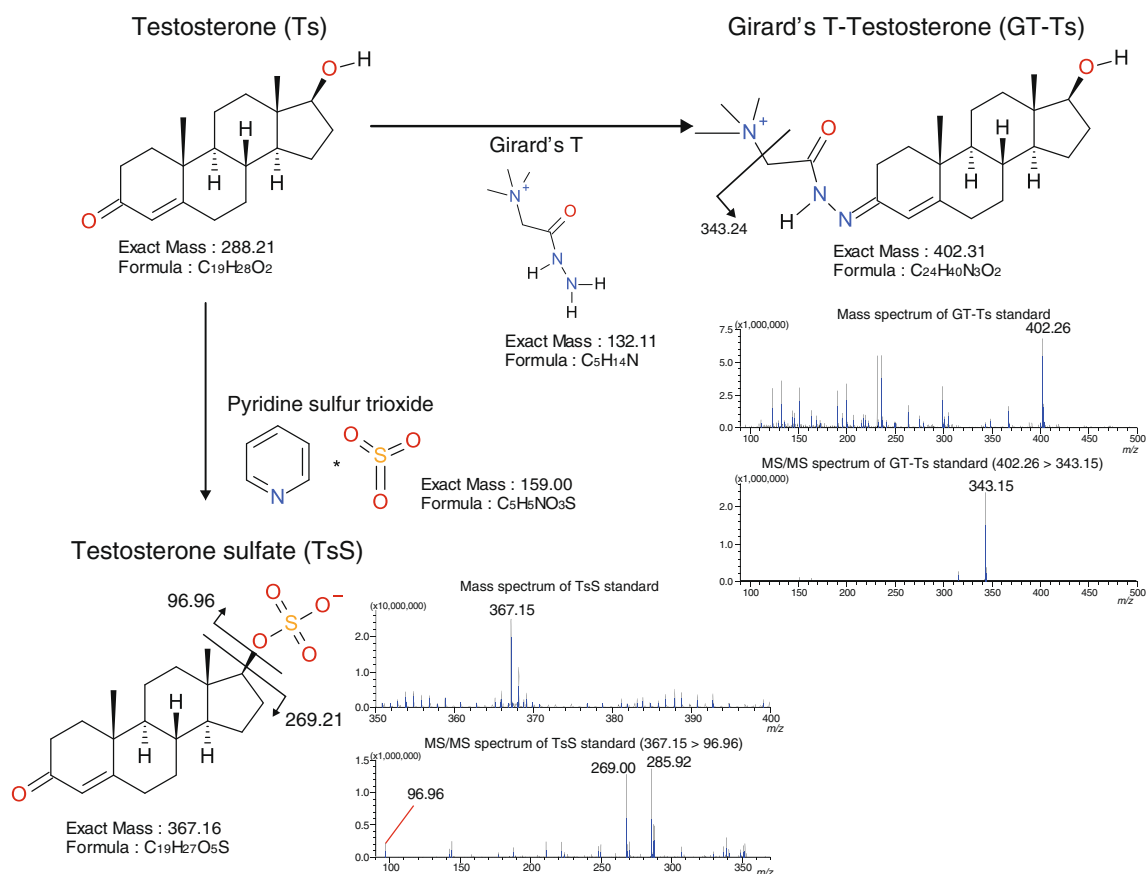


Fig. 1 Overview of reagents for on-tissue derivatization and mass spectra obtained from each derivatized standard testosterone sample. Positive ion detection for GT-Ts and negative ion detection for TsS were used. In TsS spectra, the precursor ion at m/z 367.15 and three different fragment ions

(m/z 96.96, 269.00, and 285.92) were detected. In GT-Ts, the precursor ion at m/z 402.26 and the fragment ion at m/z 343.15 with low background were detected

Therefore, these data demonstrate that the peak at m/z 289.09 was derived from the matrix and that native testosterone could not be ionized efficiently by using MALDI.

To enhance the signal-to-noise ratio for tissue measurement, we performed product ion mass spectrometry. With TsS, the peaks were expected to be detected at m/z 96.96, 269.21, and 287.20 (loss of SO_3^-) (Fig. 1). This peak pattern indicates that detection sensitivity will become lower due to the peak split. On the other hand, the MS/MS spectrum of GT-Ts provided only the peak at m/z 343.15, which was derived from neutral loss (NL) of the trimethylamine group, was observed. Comparison of these spectra indicated clearly that GT derivatization was preferable to that by pyridine sulfur trioxide with respect to detection sensitivity.

In addition to sensitivity, tissue damage during sample preparation should also be evaluated. We next examined the tissue surface after sample preparation. As shown in Fig. 2, many cracks and serious tissue shrinkage were observed between seminiferous tubules only when the tissue was treated with pyridine sulfur trioxide (Fig. 2a). It is conceivable that

this tissue damage was caused by the pyridine. In addition, no significant fragment peaks were not observed on the TsS tissues (data not shown). On the other hand, treatment of the tissue with GT preserved the original structure of seminiferous tubules in testes (Fig. 2b). Taken together, our data indicated that GT derivatization should be chosen and employed for further experiments.

To determine the optimal conditions for GT derivatization, we performed GT derivatization on tissue instead of standard testosterone sample. In this experiment, we used serial tissue sections, and spotted 0.1 μL prepared GT solutions in different concentration. After 90 min, matrix solution was applied to investigate target peak intensity at m/z 343.15. As the first step, the concentrations of GT were evaluated in 5–30 mg/mL in 2.5 % acetic acid. The most intense peak was observed at 10 mg/mL (ESM Fig. S2a). In the next experiment, the optimal concentration of acetic acid was determined under the constant GT concentration of 10 mg/mL. As the concentration of acetic acid was increased, the intensity of the target peak also increased, up to 10 % acetic acid (ESM Fig. S2b).

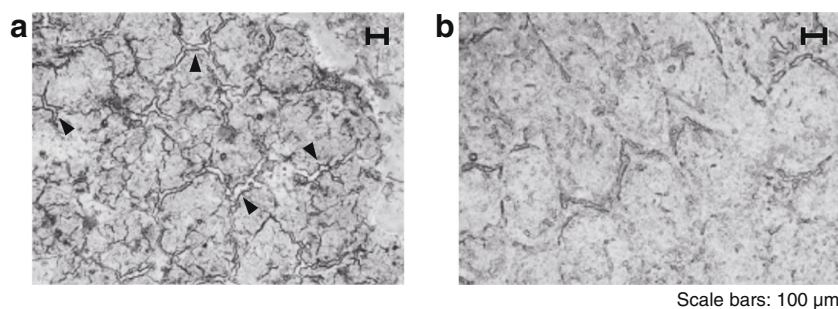


Fig. 2 Optical images to explain tissue damage due to derivatization. **a** Pyridine sulfur trioxide and **b** Girard's T reagent. *Arrowheads* indicate shrinkage or cracks in the testicular tubules. In the TsS tissue, large

numbers of cracks and tissue shrinkage were observed as compared with the GT-Ts tissue. *Scale bars*: 100 μm

Above 10 %, the intensity became constant. Therefore, the optimal conditions for on-tissue derivatization by GT were taken to be 10 mg/mL in 20 % acetic acid.

Under these conditions, IMS using on-tissue derivatized testes treated or untreated with hCG, an activator agonist of the luteinizing hormone (LH) receptor, was carried out with 15- μm pixel size. On the hCG-treated tissue section, the fragment ion peak at m/z 343.24 was clearly observed, and the specific accumulation of testosterone seemed to be visualized outside the seminiferous tubules (Fig. 3a, b). On the other hand, the peak intensity at m/z 343.24 was quite low in untreated tissue sections as compared with that of the treated ones (Fig. 3c). Testosterone signals were significantly different in the obtained MS/MS spectra (Fig. 3d). This result was also confirmed using LC-MS/MS (Fig. 3e). Our quantification results provided 5.37 ± 1.69 pg/mg in untreated testes and 1373 ± 201 pg/mL in hCG-treated testes. The difference was 256-fold higher concentration in hCG-treated testes. On the other hand, the obtained peak intensities in IMS were 1105 ± 77.4 (arb. unit) in untreated testes and $251,846 \pm 7221$ (arb. unit) in hCG-treated testes. The 228-fold change was in good agreement with LC-MS/MS results.

To determine the distribution of testosterone precisely, we performed smaller pixel size IMS at 7 μm with a high microscopic magnification view (Fig. 4a, b). Besides that in the area of accumulation, testosterone was also detected in the outer part of the seminiferous tubules under this region-of-interest (Fig. 4c, d). The optical picture clearly allowed visualization of the Leydig cell distribution among the seminiferous tubules. By overlaying the optical view on the ion distribution of testosterone, testosterone was clearly seen to have accumulated in a few Leydig cells. This is the first report of testosterone distribution with high-spatial precision and mass spectrometric specificity obtained by using the fragment ion that included structural information about testosterone for observation with the iMScope.

For testosterone, dehydroepiandrosterone (DHEA), an intermediate of testosterone synthesis, is a structural isomer,

which has a hydroxy group at C-3 and a ketone group at C-17. Due to this structure, the m/z values of the derivatized precursor ion and product ion were exactly the same, because the neutral loss of trimethylamine was detected in product ion mass spectrometry. Therefore, we had to check for the interference of DHEA presented in Figs. 3 and 4. To exclude this possibility of interference, we performed MS/MS/MS of m/z 343.24 on the tissue and compared the fragment pattern of the obtained product ion spectra with standard testosterone and standard DHEA derivatives. In Fig. 5a, the upper spectrum was obtained from the GT-Ts standard sample, and the lower spectrum, from the tissue surface. The fragment pattern was identical to testosterone. On the other hand, the main product ion peaks obtained from the GT-DHEA standard were at m/z 253.19 and 271.25 (Fig. 5b). These major peaks were not detected in the on-tissue measurement. The spectral comparison between the GT-DHEA standard and on-tissue derivatization showed that the obtained imaging results were totally derived from derivatized testosterone, because of the incomplete spectral match.

Discussion

Spermatogenesis is dependent on the maintenance of high levels of testicular testosterone and Sertoli cell activation. Accurate measurement and distribution of testosterone are required for a better understanding of spermatogenesis in normal men, and for diagnosis and treatment of disorders in testes and other genital organs. Extraction of testosterone with organic solvent for accurate measurement is not compatible with a study for its spatial distribution in testes. Although accurate measurement of testosterone is a hot argument and concern in the Endocrine Society, there are no reports on the distribution of testosterone in testes. The present study is the first report on the visualization of testosterone in testes achieved by IMS.

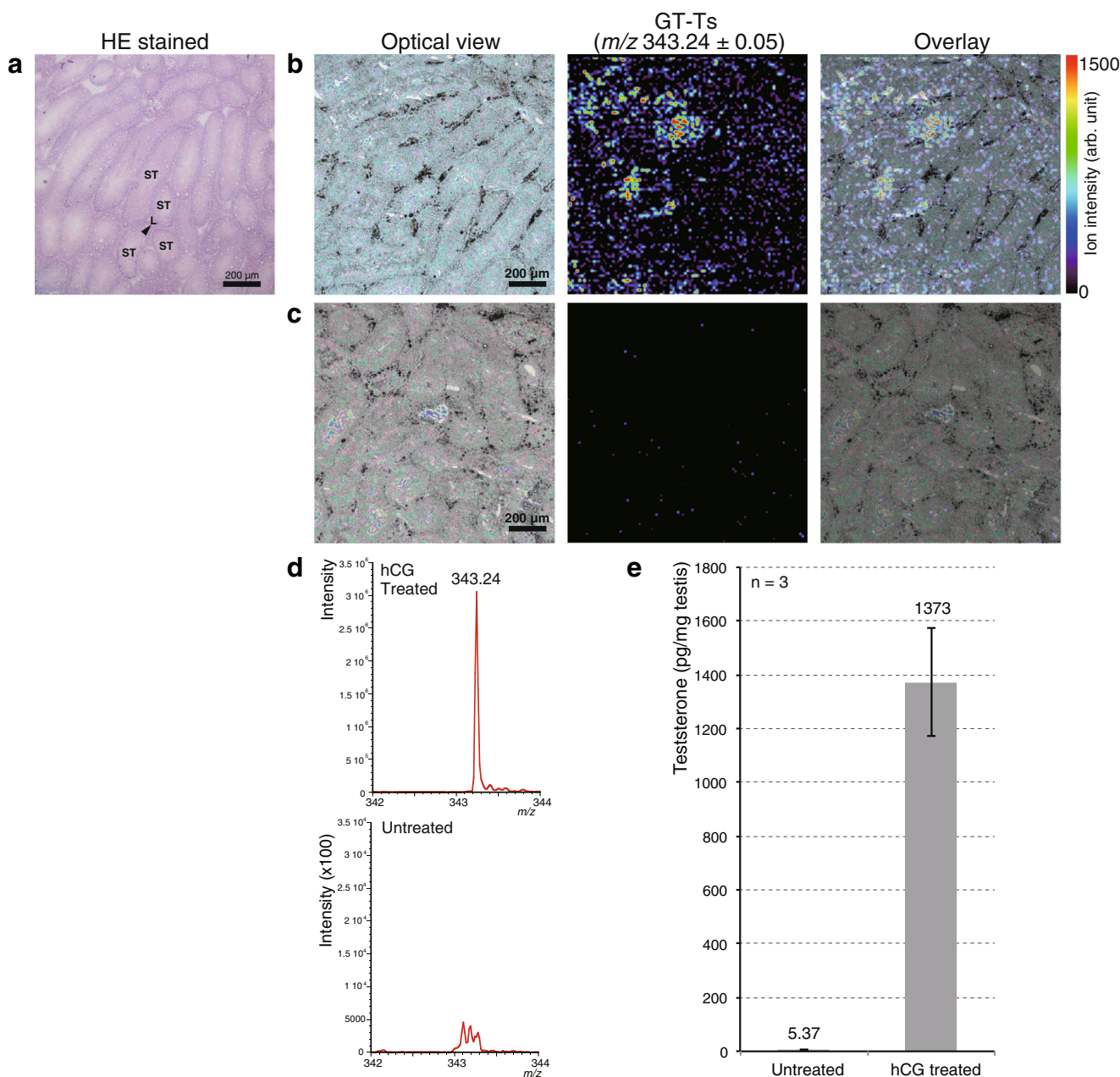


Fig. 3 Distribution of GT-Ts in mouse testes. **a** Optical picture of a hematoxylin eosin stained serial tissue section. *ST* seminiferous tubules and *L* Leydig cells. *Arrowheads* indicate Leydig cells. Distribution of GT-Ts in the mouse testes treated with **b** hCG treated and **c** hCG untreated (m/z 343.24 \pm 0.05). The pixel size of images was 15 $\mu\text{m} \times 15 \mu\text{m}$ (*scale*

bars: 200 μm). **d** Enlarged detected peaks derived from testosterone in each imaging result. **e** Quantification results of testosterone extracted from each testis tissue block. We confirmed the 256-fold higher concentration in hCG-treated testes using LC-MS/MS

Visualization of testosterone in testes by IMS

It was recently reported that the intratesticular concentration of testosterone in healthy men is 119 to 1251 ng/mL with a mean of 635 ± 368 ng/mL, as determined by using the LC-MS/MS assay, which is a more sensitive and specific means for measurement compared with immunoassays [5]. It correlated highly with serum testosterone and LH concentrations.

Since LH is well known to stimulate testosterone biosynthesis in Leydig cells, the broad variation of intratesticular testosterone seemed to be explained by a pulsatile concentration of LH. In fact, we succeeded in visualization of testosterone in Leydig cells treated with hCG, an agonist of LH receptors, but not in non-treated ones (Figs. 3 and 4). There are two pathways for testosterone biosynthesis from cholesterol, via DHEA (Δ^4 pathway) and via pregnenolone (Δ^5 pathway).

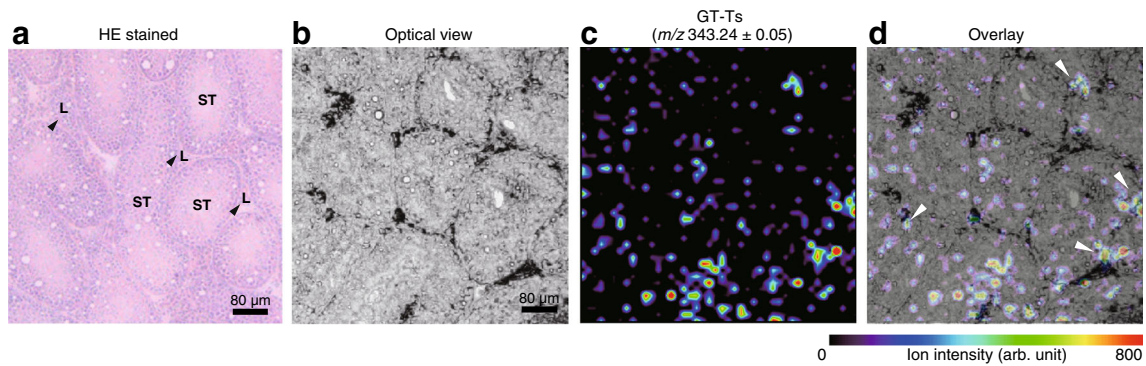


Fig. 4 High definition images (pixel size: 7 μm) of GT-Ts in the hCG-treated mouse testes. Optical picture of **a** a hematoxylin and eosin-stained serial tissue section and **b** measured tissue section. **c** Peak intensity map of

m/z 343.24 \pm 0.05 and **d** overlay with optical picture. Arrowheads indicate accumulated testosterone in Leydig cells. Scale bar: 80 μm

Circulating DHEA sulfate is postulated to serve as a systemic reservoir for testosterone biosynthesis, and it is taken up by testes, desulfated, and converted to testosterone [1]. Since testosterone and DHEA are structural isomers with the same m/z values of derivatized precursor and product ion, it was necessary to determine whether the IMS of testes was ascribed to testosterone or DHEA (Figs. 3 and 4). We performed MS/MS/MS of m/z 343.24 on testes and showed that the image of testes was derived from testosterone (Fig. 5). In steroidogenic tissues including testes, P450 side chain-cleaving enzyme, i.e., P450_{scc}, which catalyzes the conversion of cholesterol to pregnenolone, is a rate-limiting enzyme for testosterone

biosynthesis and is stimulated by LH. Because DHEA is an intermediate product of testosterone biosynthesis, its concentration would seem to have been below the detection limit even after LH stimulation.

The androgen receptor is one of the nuclear steroid receptors, and it is localized in both the cytoplasm and nucleus. In the adult male mouse testes, this receptor is expressed in Leydig cells, Sertoli cells, and most peritubular cells, but not in germ cells. The expression of androgen receptor is a function of the cycle of the seminiferous epithelium in mice [13]. Although synthesized testosterone is considered to be promptly released into the bloodstream, high-definition imaging

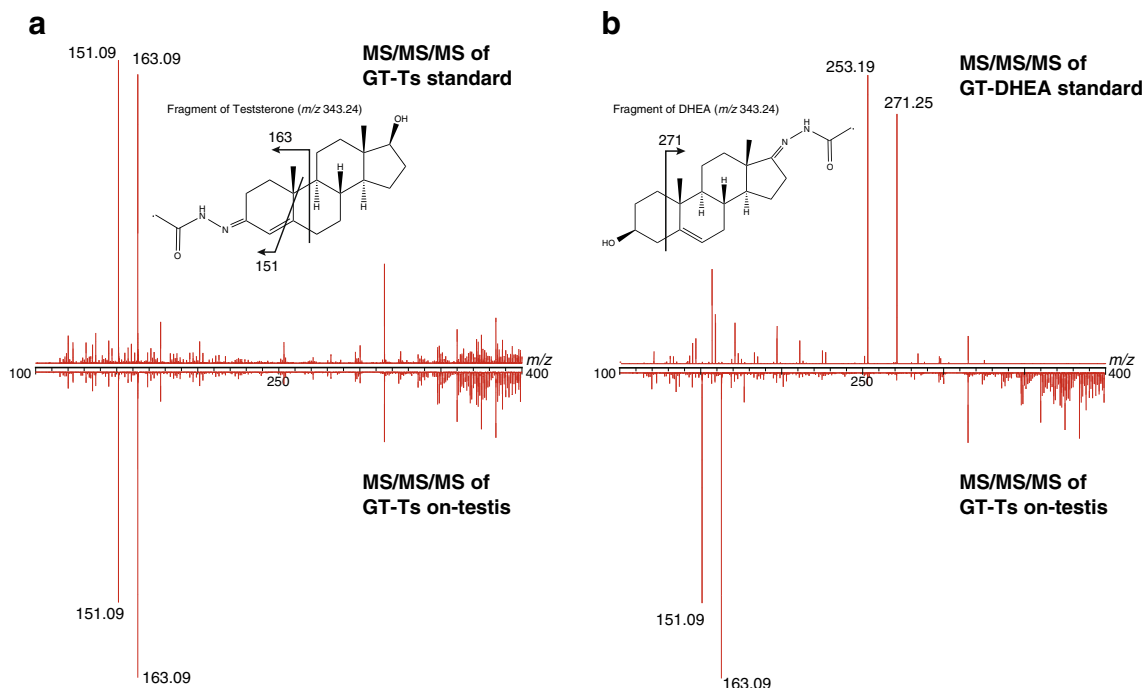


Fig. 5 Comparison of product ion spectra obtained from an MS/MS/MS experiment. **a** MS/MS/MS spectra of m/z 343.24 obtained from GT-Ts standard sample (*upper*) and on-tissue derivatization sample (*lower*). **b**

MS/MS/MS spectra of m/z 343.24 obtained from GT-DHEA (*upper*) and on-tissue derivatization sample (*lower*)

revealed that, in addition to its accumulation in Leydig cells, the derivatized testosterone signal was present, probably as a form bound to androgen receptors, in Sertoli cells of the seminiferous tubules (Fig. 4).

Fragment pattern of derivatized testosterone

In the present study, we evaluated two reagents for on-tissue derivatization. According to our sample preparation results, we concluded that GT was superior to pyridine sulfur trioxide in testosterone imaging from the aspect of tissue damage (Fig. 2). In addition to this merit, fragment patterns in MS/MS spectra of derivatized molecules should be discussed regarding the selection of derivatization reagents.

At first, both derivatized molecules would produce peaks derived from charged group (trimethylamine group and sulfate group). However, the spectra provided the no peaks derived from trimethylamine in positive ion mode and the peak derived from sulfate group with low intensity (Fig. 1). This reason was due to a property of the used type of mass spectrometer. The iMScope has the ion trap mass spectrometer as the first mass analyzer. In principle, ion trap mass spectrometers cannot trap fragment ions in the lower m/z region due to low mass cut off (LMCO). The typical low m/z boundary is below a third of the m/z value of the precursor ion. The values of LMCO of GT-Ts and TsS are approximately m/z 130 and 120, respectively. Therefore, m/z 59 ($(\text{CH}_3)_3\text{N}^+$) was not detected, and the detection efficiency of m/z 96.96 (SO_4^-) was quite low shown in Fig. 1.

Secondly, the peaks derived from NL of charged site (m/z 343.24 in GT-Ts and m/z 269.21 and 287.21 in TsS) are also important for further analysis to recognize structural isomers. If visualization is performed by using polar group ions, maintenance of the specificity of visualization is difficult. In GT-Ts reagent, the peak at m/z 343.24, which was due to the NL of trimethylamine, was clearly detected as a single intense peak even on the tissue surface (Fig. 3). If the NL moiety is clearly detected, MSⁿ ($n > 2$) can be carried out to check for the contamination by other isomers, as was shown in Fig. 5. On the other hand, the three different NL peaks were detected in MS/MS spectra of TsS standard sample. As we mentioned, the peak splitting in MS/MS spectra will become a drawback for structural isomer discrimination in IMS due to lack of peak intensity. This feature also supported to select GT reagent to visualize Ts.

Advantages of our methods in high-definition IMS

In the present study, we performed high-definition IMS of 7 μm pixel size to visualize testosterone accumulation in Leydig cells, as was shown in Fig. 4. In case of visualization of the molecular accumulation in an area with a scale of just a few micrometers, position alignment of optical views and IMS

results is strictly required. As described in the experimental section, taking optical pictures under microscopic views and ion images are able to be obtained within the same system. This feature can provide high-precision position alignment [12]. Another requirement for performing high-definition MALDI-IMS is minimization of the matrix crystal size. In our previous study [14], our matrix application method was able to create tiny (approximately 0.5 μm) matrix crystals on the tissue surface. We considered that these two advantages resulted in successful high-spatial IMS at the microscopic level. As proposed in a recent review [1], accurate mapping of the testosterone molecule in testes at the cellular level has now been achieved. IMS of testosterone will provide insights into its function in both normal and pathological states such as prostate cancer and hyperandrogenism in women with polycystic ovary syndrome.

Acknowledgments This work was supported in part by Grants-in-Aid for Scientific Research (B) (25293137 to SI) and for Challenging Exploratory Research (26670291 to SI) from the Japan Society for the Promotion of Science and by a MEXT-supported program for the Strategic Research Foundation at Private Universities (SI). We wish to thank Prof. E. Fukusaki (Osaka University) and visiting Prof. J. Iida (Shimadzu) for the use of facilities in Osaka University Shimadzu Analytical Innovation Research Laboratory. We also thank Ms. M. Suzuki for the assistance with the LC-MS/MS analyses.

Compliance with ethical standards

Conflict of interest The authors declare that they have no conflict of interest.

References

- Mueller JW, Gilligan LC, Idkowiak J, Arlt W, Foster PA The regulation of steroid action by sulfation and desulfation. *Endocr Rev.* 2015;36(5):526–63.
- Wang C, Catlin DH, Demers LM, Starcevic B, Swerdloff RS. Measurement of total serum testosterone in adult men: comparison of current laboratory methods versus liquid chromatography-tandem mass spectrometry. *J Clin Endocrinol Metab.* 2004;89(2):534–43.
- Rosner W, Auchus RJ, Azziz R, Sluss PM, Raff H. Position statement: utility, limitations, and pitfalls in measuring testosterone: an Endocrine Society position statement. *J Clin Endocrinol Metab.* 2007;92(2):405–13.
- Handelsman DJ, Jimenez M, Singh GK, Spaliviero J, Desai R, Walters KA. Measurement of testosterone by immunoassays and mass spectrometry in mouse serum, testicular, and ovarian extracts. *Endocrinology.* 2015;156(1):400–5.
- Roth MY, Page ST, Lin K, et al. The effect of gonadotropin withdrawal and stimulation with human chorionic gonadotropin on intratesticular androstenedione and DHEA in normal men. *J Clin Endocrinol Metab.* 2011;96(4):1175–81.
- Cobice DF, Mackay CL, Goodwin RJ, McBride A, Langridge-Smith PR, et al. Mass spectrometry imaging for dissecting steroid

- intracrinology within target tissues. *Anal Chem.* 2013;85(23):11576–84.
7. Higashi T, Yamauchi A, Shimada K. 2-Hydrazino-1-methylpyridine: a highly sensitive derivatization reagent for oxosteroids in liquid chromatography–electrospray ionization–mass spectrometry. *J Chromatogr B.* 2005;825(2):214–22.
 8. Sugiura Y, Zaima N, Setou M, Ito S, Yao I. Visualization of acetylcholine distribution in central nervous system tissue sections by tandem imaging mass spectrometry. *Anal Bioanal Chem.* 2012;403(7):1851–61.
 9. Shariatgorji M, Nilsson A, Goodwin RJA, et al. Direct targeted quantitative molecular imaging of neurotransmitters in brain tissue sections. *Neuron.* 2014;84(4):697–707.
 10. Shariatgorji M, Nilsson A, Kallback P, et al. Pyrylium salts as reactive matrices for MALDI-MS imaging of biologically active primary amines. *J Am Soc Mass Spectrom.* 2015;26(6):934–9.
 11. Shimma S, Takashima Y, Hashimoto J, et al. Alternative two-step matrix application method for imaging mass spectrometry to avoid tissue shrinkage and improve ionization efficiency. *J Mass Spectrom.* 2013;48(12):1285–90.
 12. Harada T, Yuba-Kubo A, Sugiura Y, et al. Visualization of volatile substances in different organelles with an atmospheric-pressure mass microscope. *Anal Chem.* 2009;81(21):9153–7.
 13. Zhou Q, Nie R, Prins GS, et al. Localization of androgen and estrogen receptors in adult male mouse reproductive tract. *J Androl.* 2002;23(6):870–81.
 14. Shimma S. Characterizations of two-step matrix application procedures for imaging mass spectrometry. *Mass Spectrom Lett.* 2015;6(1):21–5.